

**ACTA TECHNICA NAPOCENSIS**

**Series: Applied Mathematics, Mechanics, and Engineering**  
**Vol. 57, Issue II, June, 2014**

**PERFORMANCES OF THE PERMANENT MAGNET  
SYNCHRONOUS AND THE SWITCHED RELUCTANCE MACHINE  
USED IN AUTOMOTIVE TRACTION APPLICATIONS**

**Marius MOROŞANU, Liviu SOMEŞAN, Mircea RUBA, Ioan Adrian VIOREL**

**Abstract:** The goal of the present paper is to analyze comparison wise two structures of electrical machines applicable for automotive traction. The chosen machines are the permanent magnet synchronous one and the switched reluctance one. The comparison is handled by theoretical aspects, like design, analytical approach and finite element based simulations. The comparison is carried out starting from the same requirements and comparing their behavior in the same motor regimes. The performances of each machine are highlighted concluding with the advantages and drawbacks of each of them.

**Keywords:** permanent magnet, switched reluctance, comparison

## 1. INTRODUCTION

In the last decades the automotive industry is one of the main sources of air pollution and a major consumer of oil resources. Future oil depletion and environmental damage produced by the gas emissions push automobile industry to improve traction efficiency and to reduce oil consumption and pollution.

Because of this requirements, the hybrid electric vehicles have become very popular. Nowadays, it is difficult to imagine the future without hybrid electric vehicles.

As compared to the conventional machines, the hybrid electric vehicles have some major advantages such as the reduction of fuel consumption and pollution, due to the hybridization process. However, the hybrid electric vehicles have some drawbacks such as the increased cost and the architecture complexity.

These days, the technological innovations have led to the increased use of new types of electrical machines in hybrid electric vehicles

such as permanent magnet flux-switching machine.

This thesis is intended to be a comparative study between three different motors, respectively permanent magnet flux switching, permanent magnet synchronous and switched reluctance motor, in order to determine who is the most suitable machine for the hybrid electric vehicle propulsion system.

Switched reluctance machines (SRM) are one of few alternative candidates for the next HEV generation. The SRM has several attractive features, such as a simple structure, low cost, rotor robustness, high starting torque and wide speed range [1], [2].

The SRM is a doubly salient machine, as illustrated in Figure 1, with a passive rotor. It is a singly excited reluctance machine with independent phase windings on the stator [3]. The stator winding consist of coils placed on the stator poles, usually one coil on each pole. An excitation phase comprises two poles coils connected in series, usually two opposite poles, but other connections are also possible. Each phase is independent and the excitation

represents a sequence of voltage/current pulses applied to each phase in turn. The rotor structure is very simple without any windings or permanent magnets (PMs), and is made of magnetic steel laminations.

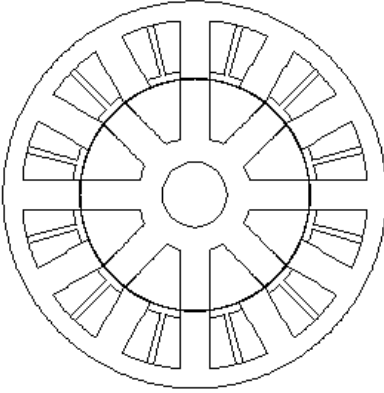


**Fig. 1** The studied SRM structure

The permanent magnet synchronous machine (PMSM) is the most suitable and the mainly applied machine type in HEV applications due to their high power density, compact size, high efficiency, and wide speed range operation[4], [5],[6],[7].

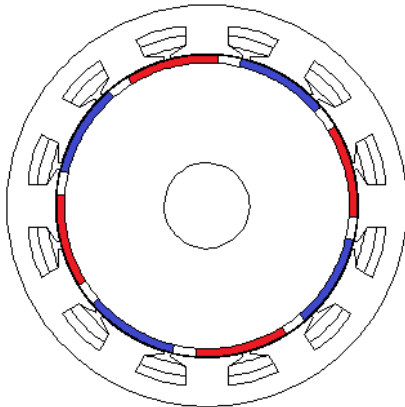


**Fig. 2** The studied PMSM structure

In PMSM, Figure 2, a three-phase balanced supply to the stator windings of a PMSM produces a sinusoidal mmf in the air gap. The rotor magnetic field produced by the PMs can be made sinusoidal by shaping the magnets and controlling their magnetizing directions. The electromagnetic torque is generated on the shaft by the interaction of these two magnetic fields created by the stator and the rotor circuits.

Surface mounted PMSMs, as illustrated in Figure 2, are compact and also rugged in

structure. In the surface mounted PMSM, the PMs are easily epoxy-glued or wedge-fixed to the cylindrical rotor. Interior PMSMs can achieve high torque and power densities, which are very attractive for HEV applications. However, since the d-axis and q-axis stator winding inductances of such machines are the same, they exhibit zero reluctance torque.

The goal of this paper is to compare two such machine in order to create an image regarding the choice for the best suitable machine for traction applications. For the comparison, analytical models are engaged as preliminary analysis, going further on to finite element analysis (FEA), to increase even more the accuracy of the obtained results and conclusions.

## 2. THE DESIGN OF THE PMSM AND SRM IN STUDY

For each of the two machines, an analytical design breviary was created having for both the same input requirements in order to obtain comparable electrical machines. From the design sheet, the machine's geometrical features are computed function of the rated requirements.

The proposed motors were designed for the same main dimensions, such as the air-gap diameter, air-gap length, stack length, and the same ratings, such as the phase voltage, number of turns per phase, phase number and rated speed.

The main dimensions of the proposed motors are listed in Table 1. As it can be seen the PMSM has the lowest outer diameter. This fact has led to the increasing of the stator coil height, respectively of the outer diameter of the motor.

The studied machines are also designed for the same output power, respectively for 30 kW. The main dimensions and the most important parameters are evinced in Table 2.

## 3. MAGNETIC RELUCTANCES AND THE FLUX DENSITIES

### 3.1. Analysis for the PMSM

The next step, after the sizing process of the PMSM is ended is to build the magnetic equivalent circuit.

Table 1.  
Main dimensions and design  
specifications of the proposed motors

	Item	Value		
		M.U	PMSM	SRM
Design specification	Air-gap diameter	m	0.159	
	Active length	m	0.159	
	Air-gap length	m	0.0007	
	Rated phase voltage	V	230	
	Rated speed	rpm	3000	
	Phase number	-	3	
	Number of turns per phase	-	36	
	Stator/Rotor pole number	-	12/8	12/8
Analytically obtained results	Rated output power	kW	30	30
	Phase current	A	57	103.5
	Stator pole pitch	m	0.042	
	Rotor pole pitch	m	0.062	
	Stator pole width	m	0.026	0.021
	Rotor pole width	m	0.05	0.024
	Stator slot opening	m	0.004	0.021
	Rotor pole opening	m	0.012	0.038
	Stator pole height	m	0.016	0.042
	Rotor pole height	m	0.004	0.046
	Stator yoke height	m	0.014	0.013
	Rotor yoke height	m	0.062	0.016
	Coil height	m	0.012	0.037
	Motor's outer diameter	m	0.221	0.2695

In this case, the proposed magnetic equivalent circuit is illustrated in Figure 3.

The following notations will be used:

$\Phi_{PM}$ ,  $R_{PM}$  – permanent magnet flux and reluctance;

$\Phi_{oPM}$ ,  $R_{oPM}$  – permanent magnet leakage flux and reluctance;

$\Phi_{mPM}$ ,  $R_{mPM}$  – leakage flux between two permanent magnets and the corresponding reluctance;

$\Phi_g$ ,  $R_g$  – air-gap flux and reluctance;

$\Phi_{og}$ ,  $R_{og}$  – air-gap leakage flux and reluctance;

$\Phi_{Ry}$ ,  $R_{FeyR}$  – rotor yoke flux and reluctance;

$\Phi_s$  – main stator flux;

$R_{FetS}$ ,  $R_{FeyS}$  – stator tooth, respectively yoke reluctance.

$F_C$  – the coercitive force;

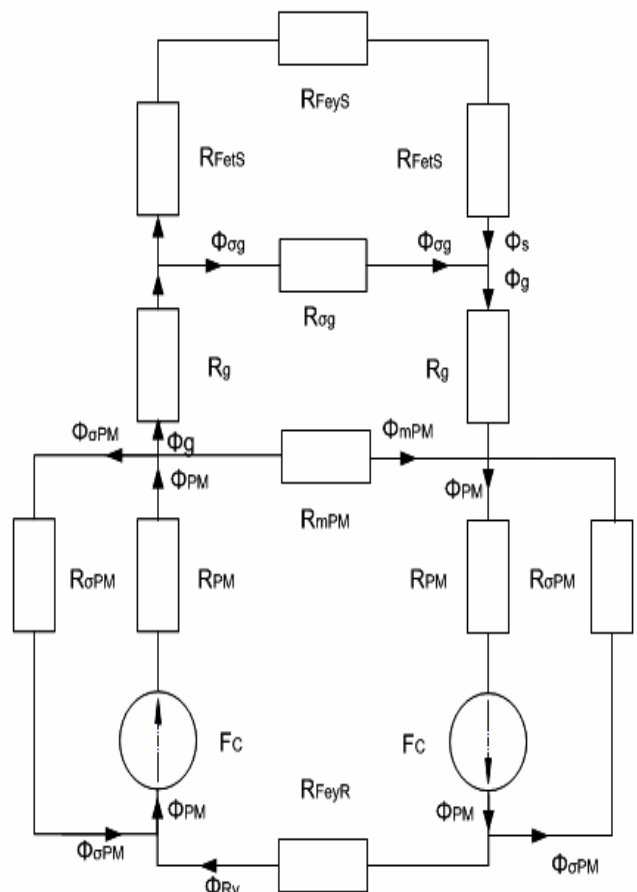


Fig. 3 The equivalent magnetic circuit

When setting up the equivalent magnetic circuit, one must consider the leakage fluxes that appear in the air-gap, between permanent magnets, respectively in the slot region. The corresponding reluctances of these fluxes are given in Table 2.

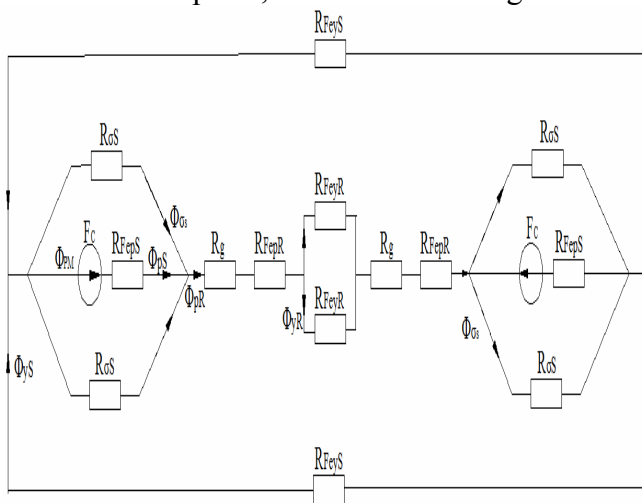
### 3.2. Analysis for the SRM

Table 2.

**Main reluctances of the magnetic equivalent circuit**

Item	Formula
Permanent magnet reluctance, $R_{PM}$	$R_{PM} = \frac{h_{PM}}{b_{PM} \cdot L_{st} \cdot \mu_{PM}}$
Permanent magnet leakage reluctance, $R_{\sigma PM}$	$R_{\sigma PM} = \frac{\pi}{\ln(1 + 2 \cdot \frac{b_{PM}}{h_{PM}}) \cdot L_{st} \cdot \mu_0}$
Leakage reluctance between two PMs, $R_{mPM}$	$R_{mPM} = \frac{1}{\mu_0} \cdot \frac{\tau_R - b_{PM}}{2 \cdot h_{PM} \cdot L_{st}}$
Air-gap reluctance, $R_g$	$R_g = \frac{g}{b_{PM} \cdot L_{st} \cdot \mu_0}$
Air-gap leakage reluctance, $R_{\sigma g}$	$R_{\sigma g} = \frac{1}{10} \cdot \frac{b_{sIS}}{h_1 \cdot L_{st} \cdot \mu_0} + 2 \cdot g$
Rotor yoke reluctance, $R_{FeyR}$	$R_{FeyR} = \frac{2 \cdot l_{yR}}{h_{yR} \cdot L_{st} \cdot \mu_{Fe}}$
Stator tooth reluctance, $R_{FetS}$	$R_{FetS} = \frac{h_1 + h_2 + h_{coil}}{b_d \cdot L_{st} \cdot \mu_{Fe}}$
Stator yoke reluctance, $R_{FeyS}$	$R_{FeyS} = \frac{l_{yS}}{h_{yS} \cdot L_{st} \cdot \mu_{Fe}}$

The magnetic equivalent circuit (MEC) model is used to calculate the no-load main flux and the flux densities in each region of the SRM. For this motor the MEC was created for the aligned position when the rotor poles are aligned with the stator poles, as illustrated in Figure 4.

**Fig. 4** MEC for aligned rotor position

As in previous two cases, in order to set up the MEC for the aligned rotor position, the

reluctances corresponding to each region of the motor were introduced and given in Table 3.

Table 3.

Item	Formula
Stator pole reluctance, $R_{FepS}$	$R_{FepS} = \frac{h_{pS}}{b_{pS} \cdot L_{st} \cdot \mu_{Fe}}$
Rotor pole reluctance, $R_{FepR}$	$R_{FepR} = \frac{h_{pR}}{b_{pR} \cdot L_{st} \cdot \mu_{Fe}}$
Rotor yoke reluctance, $R_{FeyR}$	$R_{FeyR} = \frac{l_{yR}}{h_{yR} \cdot L_{st} \cdot \mu_{Fe}}$
Stator yoke reluctance, $R_{FeyS}$	$R_{FeyS} = \frac{l_{yS}}{h_{yS} \cdot L_{st} \cdot \mu_{Fe}}$
Air-gap reluctance, $R_g$	$R_g = \frac{g_e}{b_{pR} \cdot L_{st} \cdot \mu_0}$
Stator leakage reluctance, $R_{\sigma S}$	$R_{\sigma S} = \frac{h_{coil}}{l_{coil} \cdot L_{st} \cdot \mu_0}$

$l_{yS}$ ,  $l_{yR}$  being the length of the flux paths for the stator, respectively rotor yoke and  $g_e$  being the equivalent air-gap length.

$$l_{yS} = \pi \cdot \frac{D_{out} - h_{yS}}{4} \quad (1)$$

$$l_{yR} = \pi \cdot \frac{d_{ax} + h_{yR}}{4} \quad (2)$$

$$g_e = k_{sat} \cdot g \quad (3)$$

where  $k_{sat}$  is the saturation factor.

The obtained values for the main regions of the motor are given in Table 4.

#### 4. PERFORMANCE COMPARISON OF THE PMSM AND THE SRM IN STUDY

In order to have a better comparison in terms of performances, five key factors including the torque density, efficiency, power factor, mass of the active parts and the material cost of the proposed motors, are compared in order to establish which is the most suitable motor for the proposed application.

The value of electromagnetic torque in each case is an important performance indicator to evaluate these motors from Table 1. A motor

with a higher electromagnetic torque can reach the desired speed in a shorter time than the one with a lower electromagnetic torque.

Table 4.

## Analytically calculated flux densities

Item	Formula	Calculated value (T)
Stator pole flux density, $B_{pS}$	$B_{pS} = \frac{\Phi_{pS}}{b_{pS} \cdot L_{st}}$	1.66
Rotor pole flux density, $B_{pR}$	$B_{pR} = \frac{\Phi_{pR}}{b_{pR} \cdot L_{st}}$	1.418
Rotor yoke flux density, $B_{yR}$	$B_{yR} = \frac{\Phi_{yR}}{h_{yR} \cdot L_{st}}$	1.0
Stator yoke flux density, $B_{yS}$	$B_{yS} = \frac{\Phi_{yS}}{h_{yS} \cdot L_{st}}$	1.333
Air-gap flux density, $B_g$	$B_g = \frac{\Phi_{pR}}{b_{pR} \cdot L_{st}}$	1.418

The variation of electromagnetic torque versus rotor position at constant phase current, using the numerical analysis, are illustrated in Figures 5 and 6.

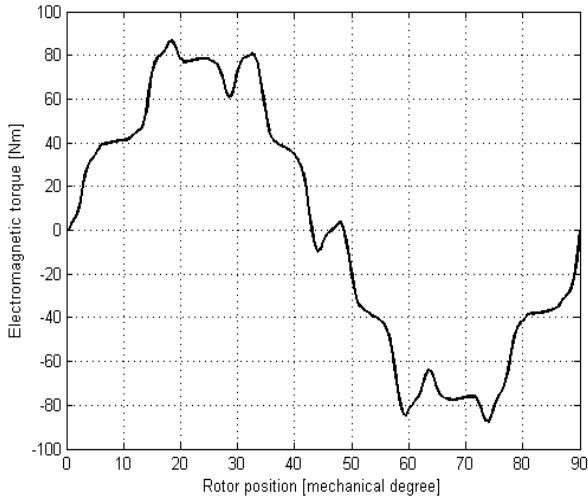


Fig. 5 Electromagnetic torque of the PMSM

In both cases the rotor was moved over a complete electric period, the corresponding

electric period being different in each case. The results are closely related to the structure of motors and to the size of permanent magnets in case of PMSM. Figures 5 and 6 show that the highest electromagnetic torque value is obtained for the PMSM, followed by the SRM with the lowest value, respectively 40 Nm.

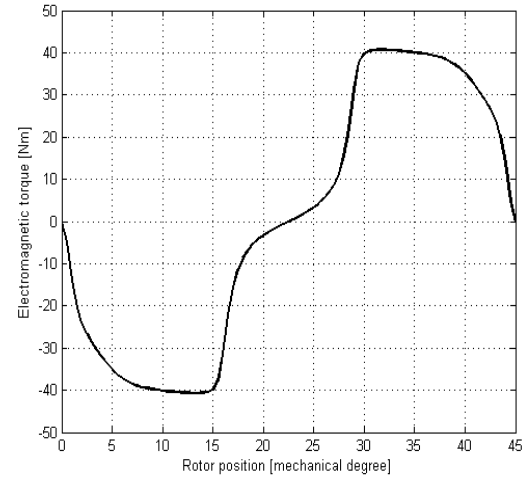


Fig. 6 Electromagnetic torque of the SRM

The equivalent electromagnetic torque in case of the PMSM is illustrated in Figure 7.

As it can be seen from Figure 7, the peak value of electromagnetic torque is approximately 87.5 Nm in case of PMSM.

After computing the electromagnetic torque and the active mass of the two considered motors, it is easy to determine the torque density.

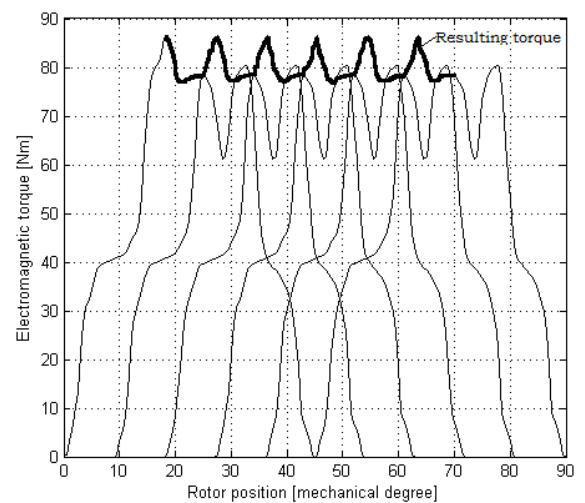


Fig. 7 The total torque of the PMSM

The corresponding torque density, efficiency, power factor, mass of the active parts and the material cost of the proposed motors are given in Table 5.

Table 5.

**Main calculated parameters of the proposed motors**

Item	Value		
	M.U	PMSM	SRM
Total losses	kW	2.46	2.678
Efficiency	-	0.916	0.822
Power factor	-	0.767	0.632
Active mass	Kg	24.66	26.3
Material costs	USD	315	133
Torque density	Nm/Kg	<b>3.55</b>	<b>1.52</b>

Analyzing Table 5, it can be observed that the PMSM has the biggest torque density, the obtained value being 3.5, more than two times higher than the one in case of SRM. Even if the volume of the PMSM is bigger than that of the SRM, the PMSM active mass is the lowest, respectively 24.66 Kg. The mass of the PMSM is lower compared to that of SRM due to the reduced weight of the rotor part. The total weight of rotor part in case of PMSM is 16.18 Kg.

However, the PMSM is the most expensive due to the necessity of a large quantity of permanent magnets, respectively 7.26 Kg, the total price of materials being 315 USD.

The necessity of a large quantity of permanent magnets and the high price of the permanents magnets used, respectively of NdFeB with the remanence flux density  $B_r = 1.2$  T and the coercive field intensity  $H_C = 910$  kA/m, made the permanent magnet motor to be more expensive comparatively with the SRM.

Permanent magnets are characterised by a number of properties, the most important when specifying a permanent magnet being the magnetic properties such as remanence flux density  $B_r$ . The influence of different remanent flux densities values (1.2 T, 0.8 T, 0.4 T) on PMSM performances is illustrated in Figures 8.

The variation of electromagnetic torque and back-emf for different values of  $B_r$  is illustrated in the above figures. It can be seen from Figure 8 that in case of PMSM, the obtained values for  $B_r = 0.8$  T differ a lot from those obtained for  $B_r = 1.2$  T.

In terms of efficiency, the choice of motor depends on the torque-speed characteristics, as was illustrated in Figure 9. The efficiency is calculated depending on the total losses and the output power of the studied motors.

The evolution of the total losses for different values of the speed is illustrated in Figure 7. It can be seen that the PMSM has the lowest losses at the rated speed, respectively 2.46 kW.

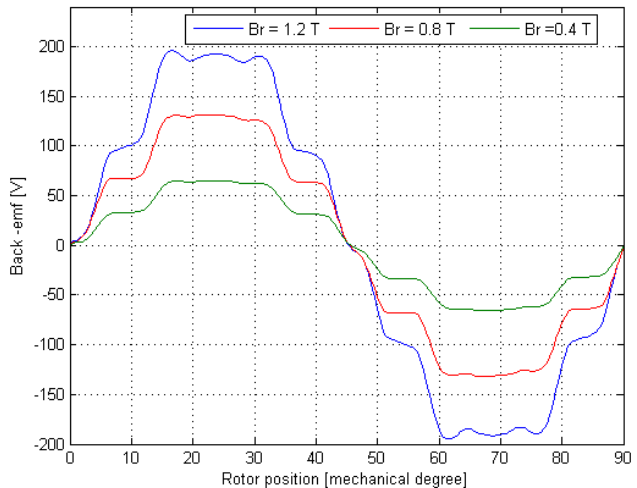
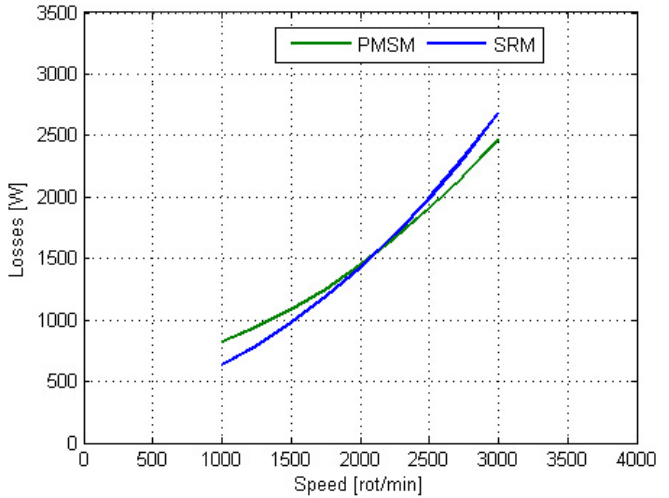
Fig. 8 . PMSM back-emf for different values of  $B_r$ 

Fig. 9 Evolution of total losses

Depending on the losses, the efficiency versus speed characteristics are given, as illustrated in Figure 10. In our case, at the rated speed of 3000 rot/min, the PMSM provides the best efficiency while the SRM has the poor efficiency.

As it can be seen from the above table, the PMSM is the most capable competitor for the SRM due to its advantages including the power factor. Also, the robust rotor structure and the variable flux control capability make this motor becoming more attractive for HEV propulsion systems.

Compared to the PMSM, the SRM has the advantage of simple and robust structure [8]. This structure does not involve permanent magnets, there being no risk of demagnetization.

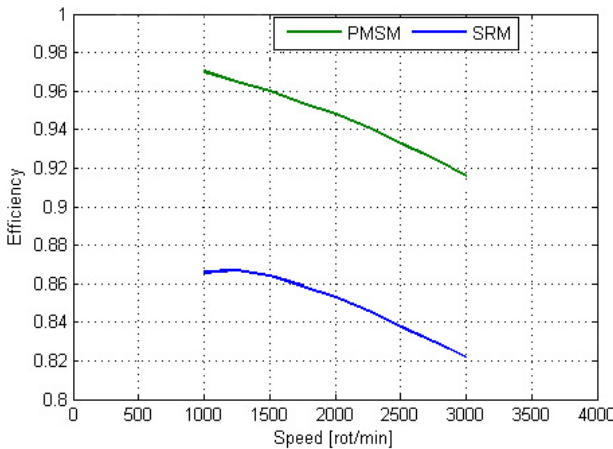


Fig. 10 Evolution of efficiency

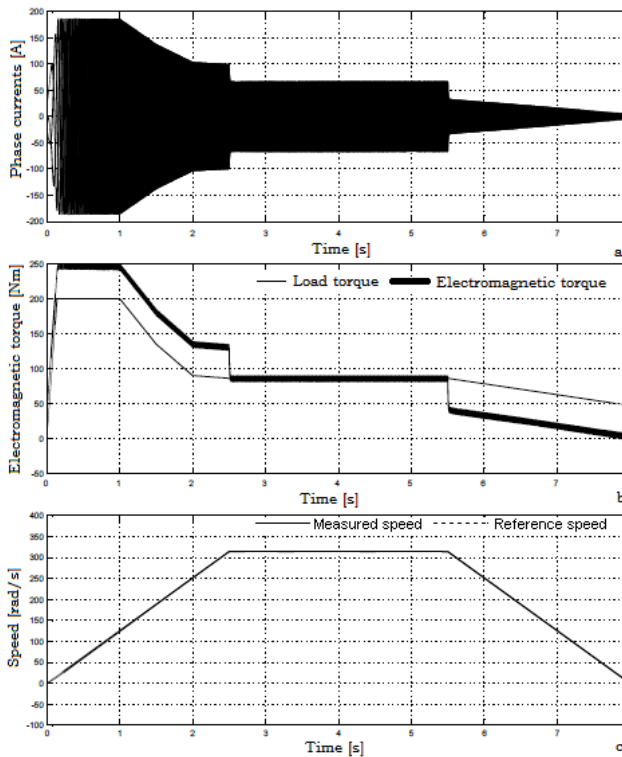


Fig. 11 PMSM dynamic simulations, evolution of the:  
 a) Phase currents  
 b) Electromagnetic torque c) Speed versus time

As mentioned before, the automotive drive applications have mainly three requirements:

1. High starting torque;
2. A certain highest speed and adequate accelerating;
3. Reduced noise and vibrations.

The first aspects are evinced in the transient regime study [9]. In the case of PMSM the rotor flux oriented vector control was involved. For such motors the control is very important to determine their behavior. Therefore, a dynamic simulation was performed at the imposed reference speed of 314 rad/s, corresponding to 3000 rot/min. In this case the load torque is not constant, a load torque profile being considered. The results of the dynamic simulations for the proposed PMSM are illustrated in Figure 11.

In automotive drive case the load torque is not constant. From this reason the load torque profile is considered. In both cases, the peak value of load torque was considered over 200 Nm.

As it can be seen from the figures, in the case of PMSM the electromagnetic torque drops to zero at the end of the speed cycle, when the speed is zero.

In conclusion, even if the SRM is suitable for the mainly applied motor type in HEV applications, the obtained results tend to promote the PMSM as a possible best solution.

## 5. CONCLUSIONS

The goal of the paper made an evaluation of the studied motors regarding their applicability on hybrid electric vehicles. Based on the results obtained in the study, a comparison is done and the obtained results tend to promote the PMSM as the best solution, despite of its high cost of the materials.

In the study several analytical and FEA based studies are engaged in order to prove the validity of the study. This comes as an addition to the actual status of the research in the field of HEVs. This is nowadays a serious trend due to the possibility of changing the supply of the vehicles from petrol based fuels to electrical energy.

In conclusion, the study reached its objectives: to offer an overview of the main

electrical motors used for hybrid electric vehicle propulsion systems.

Future studies involve advanced control strategy comparisons for the two types of motors. It is well known that there are several methods for controlling both the SRM and the PMSM in order to increase efficiency, minimize torque ripples and increase the safety in operations.

Also another important future vision regards the possibility of studying the noise and vibration aspects. It is known for example that the SRM has an increased noise during operation, this being uncomfortably for the passengers [10]. The solution for this problem is a special control strategy that silences the machine during operation. This control is so called current profiling method. It is able to minimize the torque characteristic's ripples while operating at lower noise factors.

## REFERENCES

- [1] Henneberger, G., Viorel, I.A., "Variable reluctance electrical machines", Shaker Verlag, Aachen, Germany, 2001.
- [2] Rahman, K.M., Fahimi, B., "Advantages of switched reluctance motor applications to EV and HEV: design and control issues," IEEE Trans. on Ind. Appl., vol.36, no.1, pp.111-121, 2000.
- [3] Husain, I., "Electric and hybrid vehicles design fundamentals", CRC press LLC, 2003.
- [4] Finken, T., Felden, M., Hameyer, K., "Comparison and design of different electrical machine types regarding their applicability in hybrid electrical vehicles", Proceedings of 18th International Conference on Electrical Machines ICEM 2008, pp. 1-5, Vilamoura, Portugal, 2008.
- [5] Wang, T., Zheng, P., Cheng, S., "Design characteristics of the induction motor used for hybrid electric vehicle", IEEE Transactions on Magnetics, vol.41, no.1, pp.505-508, 2005.
- [6] Yabumoto, M., Kaido, C., Wakisaka, T., Kubota, T., Suzuki, N., "Electrical steel sheet for traction motors of hybrid/electrical vehicles", Nippon Steel Technical Report, No.87, July 2003.
- [7] Zeraoulia, M., Benbouzid, M.E.H., Diallo, D., "Electric motor drive selection issues for HEV propulsion systems: a comparative study", IEEE Transactions on Vehicular Technology, vol.55, No.6, pp. 1756-1764, 2006
- [8] Fodorean, D., Popa, D.C., Jurca, F., Ruba, M., "Optimizing the design of radial/axial PMSM and SRM used for powered wheel-chairs ", World Academy of Science, Engineering and Technology, vol.59, pp. 120-125, 2011.
- [9] Ruba M., Fodorean D.: "Analysis of Fault-Tolerant Multiphase Power Converter for a Nine-Phase Permanent Magnet Synchronous Machine", IEEE Trans. On Industrial Applications, Vol. 48, no. 6, pp. 2092-2101, ISSN: 0093-9994, 2012
- [10] Ruba M., Viorel I.A., Szabó L.: "Modular stator switched reluctance motor for fault tolerant drive systems", IET Electric Power Applications, vol. 7, no. 3 (March 2013), pp. 159-169, 2013, ISSN: 1751-8660).

## Performanțele mașinii sincrone cu magneți permanenți și a mașinii cu reluctanță variabilă folosite în industria auto

**Rezumat:** Scopul lucrării curente este analiza la nivel comparativ a două mașini electrice, folosite în industria auto. Mașinile alese sunt cea sincronă cu magneți permanenți și cea cu reluctanță variabilă. Compararea se realizează asupra aspectelor teoretice, cum ar fi proiectarea, abordarea analitică și simularea bazată pe metoda elementelor finite. Compararea se efectuează pornind de la aceleași cerințe, comparând modul de comportare în regimul motor. Performanțele fiecărei mașini sunt evidențiate pe baza avantajelor și dezavantajelor fiecăreia.

**Marius MOROSANU**, PhD. Student, Technical University of Cluj Napoca, Department of Electrical Machines and Drives, mariuself007@yahoo.com, 0624-444444, 0744531488;

**Liviu SOMESAN**, Doctor, Assistant Lecturer, Technical University of Cluj Napoca, Department of Electrical Machines and Drives, mircea.ruba@mae.utcluj.ro, 0624-444444 ;

**Mircea RUBA**, Doctor, Assistant Lecturer, Technical University of Cluj Napoca, Department of Electrical Machines and Drives, mircea.ruba@mae.utcluj.ro, 0624-444444;

**Ioan Adrian VIOREL**, Doctor, Professor, Technical University of Cluj Napoca, Department of Electrical Machines and Drives, Ioan.Adrian.Viorel@mae.utcluj.ro, 0624-444444.